Journal of Applied Polymer Science

Hydrolysis of part of cassava starch into nanocrystals leads to increased reinforcement of nanocomposite films

Élia Karina de Carvalho Costa,[1] Carolina Oliveira de Souza,[2] Jania Betânia Alves da Silva,[3] Janice Izabel Druzian[2]

[1]Postgraduate Programme in Food Science, Federal University of Bahia, College of Pharmacy, Barão de Jeremoabo, Salvador BA 40170-110, Brazil

[2]College of Pharmacy, Barão de Jeremoabo, Federal University of Bahia, Salvador BA 40170-110, Brazil

[3]Engineering Mechanical College, Federal University of Recôncavo of Bahia, Rui Barbosa Cruz das Almas BA 44380-000, Brazil

Correspondence to: J. I. Druzian (E-mail: druzian@ufba.br)

ABSTRACT: This article reports on using cassava starch nanocrystals (CSN) to strengthen nanocomposite films from the same matrix. CSN were obtained by acid hydrolysis. Nanocomposite (starch:glycerol:CSN/4.0:2.1:1–10 wt %) were processed by casting and the films were characterized. The CSN (30% yield) presented minimally clustered globular forms, 45 to 178 nm in diameter, with a crystalline index of 46%. Water-vapor transmission rate, tensile strength, and elastic modulus of the films were influenced by the linear effect of CSN concentration ($R^2 = -0.92$, 0.91, 0.99, respectively), while the other parameters resulted in quadratic relations |0.69–0.96|. The film with 10% CSN presented a 43% reduction in water vapor permeability, associated with increases of 200% in traction resistance, and 616% in elasticity modulus, compared with the control. The hydrolysis of part of the cassava starch into nanocrystals resulted in a reduction in permeability and nano reinforcement of the films due to good compatibility and interaction between both, without influencing biodegradability. © 2017 Wiley Periodicals, Inc. J. Appl. Polym. Sci. **2017**, *134*, 45311.

KEYWORDS: biodegradable; mechanical properties; packaging; starch nanocrystals

Received 4 January 2017; accepted 18 May 2017

DOI: 10.1002/app.45311

INTRODUCTION

Interest in using biodegradable materials has increased due to the potential applications and the possibility of contributing to a reduction in environmental problems. In this context, the development of biodegradable matrices for packaging materials as substitutes for polymers of petrochemical origin is an emerging field.[1,2]

The use of biopolymers, such as proteins and polyssacharides, for preparing biodegradable films and edible coatings, generates innovative possibilities.[3] In this aspect, starch represents one of the most promising, due to its renewable nature, high availability, low cost, biodegradability, and a relatively reactive surface.[1,2,4,5]

Starch films are isotropic, odorless, insipid, colorless, nontoxic, and biologically degradable. However, there are strong limitations, due to their low traction properties and high permeability to water vapor when compared to conventional nonbiodegradable packaging materials,[1] due to their hydrophilic nature and sensitivity to humidity, which are difficult factors to control.[6]

One alternative for improving the mechanical and barrier properties of starch films is the use of nanocrystals as reinforcement agents.[1,7,8] Starch nanocrystals are crystals resulting from the rupture in the semicrystalline structure of the amorphous parts of starch granules.[4] When the reinforcement is derived from the same material as the matrix, such as starch nanocrystals dispersed in starch films, there is the possibility of better compatibilization.[9] As a consequence of nanosized crystals, their incorporation into small amounts produces significant improvements in properties with increases in the tensile strength and the elastic modulus.[2,4,7]

Starch nanocrystals from different sources can be used to reinforce various types of matrices, which along with the low cost, could enable a simple method of production.[5,10,11] But, the source of starch and process for obtaining it can result in differences both in nanocrystal performance and resulting nanocomposites.[2,4,11]

Recent studies have reported that nanoscale starch particles could be readily prepared from starch granules, which have

unique physical properties.[9,11] However, there are no articles reporting on the influence of adding cassava starch nanocrystals (CSN), without modifications, into polymeric matrices of the same source.

The aim of this article was to produce and characterize CSN for using them in developing flexible films from the same polymeric matrix, and evaluate the effect of the concentration of these nanocharges over the properties of the resulting nanocomposites. Thus, cassava starch-based nanocomposites incorporated with starch nanocrystals extracted from same source were developed. Although the resulting materials showed improved mechanical properties upon the addition of nanocrystals, similarly to previous reports, we also investigated the effects of this nanosized filler on the morphology as well as the swelling, thermal, and water barrier properties of the nanocomposites. Indeed, enhanced water barrier and thermal properties were achieved as well.

EXPERIMENTAL

Material

Cassava starch—Cargill Agrícola SA, Brazil (amylose content: 17%; amylopectin content: 83%; gelatinization temperature: 58 °C), glycerol (Labsynth, Brazil), and other analytical grade reagents (Vetec Quimica-Brazil).

CSN and Nanocomposites Preparation

The CSN were prepared by adding a solution of sulfuric acid (3.16*M*) in starch at a concentration of 0.15 g/mL. Thus, approximately 36 g of starch were diluted in 250 mL of H_2SO_4, according to the method of Angellier *et al.*,[12] the mixture remained in orbital (TECNAL, TE-0851) agitation (100 rpm/40 °C/5 days). After hydrolysis, the suspensions were washed using successive centrifugations (15,700 g/10 °C/15 min—HITACHI, CR22GIII) in distilled water until neutrality. Subsequently, the aqueous suspensions of CSN were stored at 4 °C after adding several drops of pure chloroform. The recovery yield of starch hydrolyzates after acid hydrolysis was calculated as the percent ratio of precipitated solids after centrifugation (10,000 rpm, 10 min) based on the initial weight of starch dry solids.[13] The hydrolysis yield (wt %) was calculated as the ratio between the weight of freeze-dried hydrolyzed particles and the initial weight of native granules for an aliquot of 100 mL taken in the 500 mL of hydrolyzed suspensions. It was verified that these aliquots were representative of the entire volume of 500 mL.

Nanocomposites were prepared from the film-forming solutions, by *casting*, mixing an appropriate amount of CSN aqueous suspension (0.5–10 wt %, relative to the dry total mass, starch + plasticizer + nanocrystals) with cassava starch (4 wt %) and glycerol as plasticizer (2.0 wt %). A control formulation was made without the addition of nanocrystals. The mixture was heated from room temperature at a heating rate of 3.0 °C min^{-1} under mechanical stirring during 15 min until gelatinization, which occurred at ~70 °C. After gelatinization, the gel was degassed for 30 min placed under ultrasonic bath to remove the bubbles, 40 g of the filmogenic solution was weighed into polystyrene dishes and dried in an oven with air circulation (35 ± 2 °C) (TECNAL, TE-394/I) for 16 to 20 h. The films were conditioned (75% RH, 23 °C) in desiccators with a saturated solution of NaCl for 10 days before being characterized.[1,7]

Characterization of CSN and Nanocomposites

Microstructure. The suspensions of CSN were analyzed by transmission electron microscopy, (FEI Tecnai G2-Spirit), operating in the bright field mode at 80 kV to determine the morphology of the starch nanocristais. CSN and uranyl acetate solutions equal volumes (2% v/v) were prepared. 10 μL of the mixture was dispensed in a 400 mesh copper grid, allowed to stand for 30 to 60 s.

Surface Charge and X-ray Diffraction Analysis. The surface charge of the CSN was determined by electrophoretic mobility measurements on equipment Zetasizer Nano ZS (Malvern) (NBTC, 2013) in triplicates.

The crystalline structure of CSN were analyzed (in triplicates), with freeze-dried samples by using an X-ray diffractometer (X'pert APD, Philips, The Netherlands) with Cu-Kα radiation (λ = 1.5433 Å) at a target voltage and current of 40 kV and 30 mA, respectively. The scanning range and rate were 5 to 50° (2λ) and 1.0°/min. The relative crystalinity index (RCI) was determined.[14]

Thermal Characterization of CSN and Nanocomposites. The glass transition temperature (T_g) and melting temperature (T_m) were determined by differential scanning calorimetry (DSC) (Perkin Elmer, DSC 7). Scanning was performed in triplicates, at −100 to 250 °C at a rate of 10 °C/min and a flow N_2 10 mL/min.

The thermogravimetric analysis (TGA) were performed in a thermal analyzer (Shimadzu, DTG-60), by heating the sample from 25 to 700 °C at 30 °C min^{-1} in nitrogen atmosphere. The samples were analyzed in triplicates.

Swelling and Solubility of Nanocomposites. To determine the swelling in distilled water, the nanocomposite films were cut into disc shape (17 mm). After immersion (0–120 min) at 37 °C, the swelling percentage were determined gravimetrically,[15] eq. (1).

$$\text{Swelling (\%)} = \frac{W_1 - W_0}{W_0} \times 100 \quad (1)$$

W_0 and W_1 were initial dry mass and the mass of the sample after immersion for a specified period, respectively.

For desolubility, the samples were submerged in distilled water for 24 h at 37 °C and the weight loss percentage determined,[15] eq. (2).

$$\text{Solubility (\%)} = \frac{W_2 - W_0}{W_0} \times 100 \quad (2)$$

W_0 and W_2 were dry weight of the samples before and after submersion in distilled water, respectively.

The swelling and solubility determination of the samples were analyzed in triplicates.

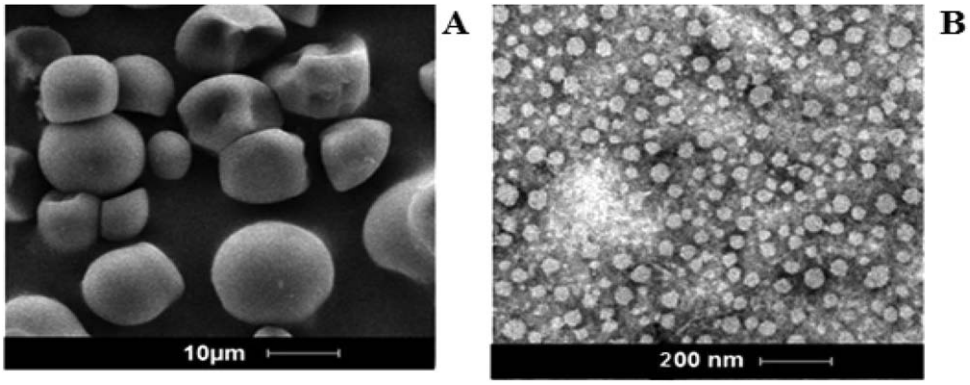

Figure 1. Micrographs of native cassava starch (A) and cassava starch nanocrystals (B).

Water Activity and Moisture. Water activity of the films were made in AQUALAB LITE and the moisture content by the gravimetric using a moisture analyzer infrared (MX-50, A&D Company), in triplicates.

Thickness, Water Vapor Transmission Rate (WVTR), and Water Vapor Permeability (WVP). The thickness was determined by micrometer (Mitutoyo, Tokyo, Japan) (1 μm resolution). Six measurements were randomly taken at different locations for each specimen, and the mean value is reported. The WVTR and WVP of the nanocomposite were determined in triplicates[16] using eqs. (3) and (4).

$$\text{WVTR}\ (\text{g.m}-2.\text{h}-1) = \frac{G}{t\ \text{x}\ \text{Ap}} \quad (3)$$

$$\text{WVP}\ (\text{g}-1.\text{s}-1.\text{Pa}-1) = \frac{\text{WVTR}\ \text{x}\ e}{S\ \text{x}\ (R1 - R2)} \quad (4)$$

WVTR, vapor permeation rate of water; G, the mass change; t, time, A_p, area permeation; WVP, permeability to water vapor; e, film thickness; S, saturation pressure of water vapor at the test temperature; $R1$ and $R2$, relative humidity of the air in each of the sample surfaces.

Mechanical Properties of Nanocomposites. The mechanical properties were obtained using an Emic Universal Testing Instrument (Model DL2000), operated as specified in ASTM D638–9.[17] Film strips of 8 cm × 2.5 cm^2 (length × width) were cut from each preconditioned sample and mounted between the grips of the machine. The initial grip separation and crosshead speed were set to 50 mm and 5.0 mm/min, respectively and the load cell of 500 N. At least 10 replicates of each specimen were averaged together.

Biodegradability of Nanocomposites. The biodegradability of the films was conducted, in triplicates, for a period of 17 weeks according to Leite *et al.*[18] The simulated soil in the test was prepared by mixing equal parts of fertile soil with low clay content, dry beach sand and sieved (40 mesh), and manure dry horse in the sun for 2 days.[19]

Statistical Analysis

Analysis of variance was performed and significant differences ($P < 0.05$) were observed by F test, the averages of each response were compared by Tukey test, 5% significance level, using the computer program SPSS 17.0 (SPSS Inc., 160, Chicago, IL).

The effects of nanocrystals concentrations on quantitative parameters were calculated by the regression model, taking into account the level of significance and the coefficient of determination (R^2). The degrees of freedom of the factors were deployed in their linear and quadratic components to choose the regression model that best described the observations.

RESULTS AND DISCUSSION

CSN Characterization

The morphological analyses show original starch granules with a 6 to 17 μm size distribution and approximately spherical geometry [Figure 1(A)]. The hydrolysis of this starch with 3.16M H_2S0_4 (100 rpm/40 °C/5 days) resulted in CSN with 47 to 178 nm, spherical geometry [Figure 1(B)], and approximately 30% of yield. The values for size and yield are in accordance with those reported for CSN produced by acid hydrolysis[20] and gama radiation.[2,21]

CNSs obtained by the study group using gama radiation also presented a spherical geometry, with a diameter around 50 nm and the presence of clusters.[2] Kim *et al.*[11] reported that nanocrystal performance and size depend on the starch source, on the type of hydrolysis or process, on the nature and concentration of acid, and on the time and temperature of the process.

Starch nanocrystals can cluster due to the greater surface area and resulting increase in hydrogen bonds between —OH.[5,25] The potential zeta of the nanocrystals is a property used to characterize the surface charge, influenced by their composition and dispersion in the aqueous medium. The measurements were used to estimate the repulsive electrostatic forces among particles and provided an idea of the stability of the nanocrystals suspension. CSN showed an average zeta potential of -4.30 ± 0.11 mV, which is attributed to the presence to negatively charged sulfate groups on the nanocrystal surface. During acid hydrolysis via sulfuric acid, acidic sulfate groups are likely formed on the nanoparticle surface. This creates an electric double layer repulsion between the nanoparticles in suspension, which plays an important role in their interaction with a polymer matrix and with each other.[26] The use of H_2SO_4 reduced the possibility of the agglomeration of starch nanocrystals and limits their flocculation in aqueous media [Figure 1(B)]. This feature is important for processing of nanocomposite materials.

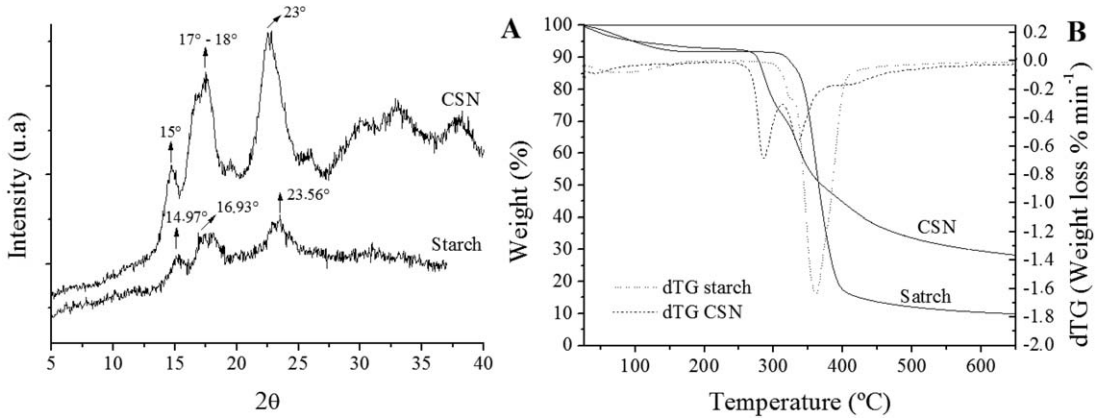

Figure 2. X-ray diffraction (XRD) (A), thermogravimetric analysis (TGA), and differential thermogravimetry (DTG) curves (B) of native cassava starch and cassava starch nanocrystals (CSN).

The X-ray diffraction profiles of native cassava starch and CSN are quite similar; however, it can be observed that the acid treatment results in the narrowing and increasing of the peaks intensity, most probably due to the higher crystallinity level of the hydrolyzed starch compared to the original cassava starch. [Figure 2(A)]. Cassava starch presents low intensity peaks in $2\theta = 14.97°$, 16.93°, and 23.56°, and CSN has single broad peaks at $2\theta = 15°$, 17 to 18.1°, and 23°, indicating a type A crystalline arrangement for both. These peaks are in agreement with Shahrodin *et al.*,[27] that analyzed the influence of different concentration of sulfuric acid in obtaining CSN.

RCI of native cassava starch (22%) was increased to 46% in the CSN. The increase in RCI after the acid hydrolysis of starch results in a disorganization of suspensions, due to incomplete removal of amorphous regions, and the less ordered superficial chains.[28] The RCI of starch nanoparticles varies from 34.6% to 45.9%, depending on the hydrolysis conditions (acid or enzymatic, time, temperature, and starch source).[13] The RCI of CSN obtained with sulfuric acid (3.16*M*/100 rpm/40 °C/5 days) lies on the upper limit of this interval. For CSN obtained by gamma radiation, the crystalline percentage ranged from 45% to 53%.[21]

CSN obtained with different concentrations of sulfuric acids showed strong reflection at 2θ about 15.1° and 23° and unresolved doublet at 16.9° and 18.1° 2θ, which was very close to a type X-ray diffraction pattern. However, B type peaks became sharper due to the increasing crystal structure formed by the gradual addition of acid concentration. The disappearance of the characteristic A type peak pattern and appearance of typical B type diffraction peak indicated that crystal type of NCS starch changed during hydrolysis process.[27]

From the curves of DSC were identified the values for glass transition temperature (T_g), gelatinization temperature (T_p), and melting temperature (T_m). The T_g of the starch and the CSN were −19.82 and −23.63 °C, respectively. The T_p was 63.43 °C for starch and 96.57 °C for CSN, indicating that acid hydrolysis results in an increase in this parameter associated with an increase in RCI [Figure 2(A)], conferring a greater structural stability to nanocrystals. The T_m was 230 °C for starch and 227 °C for CSN, indicating that the hydrolysis of the starch (a part) did not alter this parameter. Freitas *et al.*[29] reported 63.5 °C for T_p of cassava starch, and Sun *et al.*[22] reported 76 to 92 °C for corn starch nanoparticles, similar to the values obtained.

The TGA/differential thermogravimetry [Figure 2(B)] curves show that cassava starch and the respective nanocrystals present two mass loss events. The first event, associated with loss of moisture, occurred at 118.07 °C with a ∼12% loss of mass for the starch, and at 59.35 °C with a ∼9.60% loss of mass for the CSN. The initial temperature of thermal decomposition of the starch was 387.8 °C with a 77.00% loss of mass, and that of the CSN was 267.67 °C with a 60.79% loss of mass, which indicates lower CSN thermal stability. The T_{onset} of decomposition of native starch (318 °C) is higher than that of the respective CSN (269–295 °C), which could favor processing the nanocomposites by extrusion.[22] We believe that H_2SO_4 decreases the thermal stability of nanocrystals due to the presence of superficial sulfate groups.[4]

The Effect of CSN Concentration on Nanocomposite Film Properties

Nanocomposite films of cassava starch:glycerol:CSN (4:2.1:0.1–10 wt %), obtained via casting were characterized to evaluate the effect of nanocrystal (CSN) incorporation on the properties of films.

For degree of swelling the two-stage water absorption pattern was evident in all nanocomposites [Figura 4(A)]. At shorter times ($t < 10$ min) the absorption kinetics are fast, whereas after that a slower absorption process follows, reaching a plateau. The control film presented the highest percentage of swelling in 120 min (367%), whereas the films with 0.5% to 3.0% CSN varied between 306% and 348%. The degree of swelling is proportional inversely at CSN concentration during the 120 min the exposition ($R^2 = 0.93$ in equilibrium). The formation of the network due to the good interaction and dispersion of the CSN and the starch matrix, resulted in a higher swelling capacity at the beginning of the contact of films with water until stabilization of the expansion capacity. The phenomenon can be ascribed to the formation of a rigid three-dimensional starch nanocrystal network (due to the strong hydrogen bonding between the starch particles which prevents swelling of the matrix).[6]

Silva *et al.*[1] reported that solubility of films of cassava starch:eucalyptus cellulose nanocrystal (0.1%–5.0%) after equilibrium

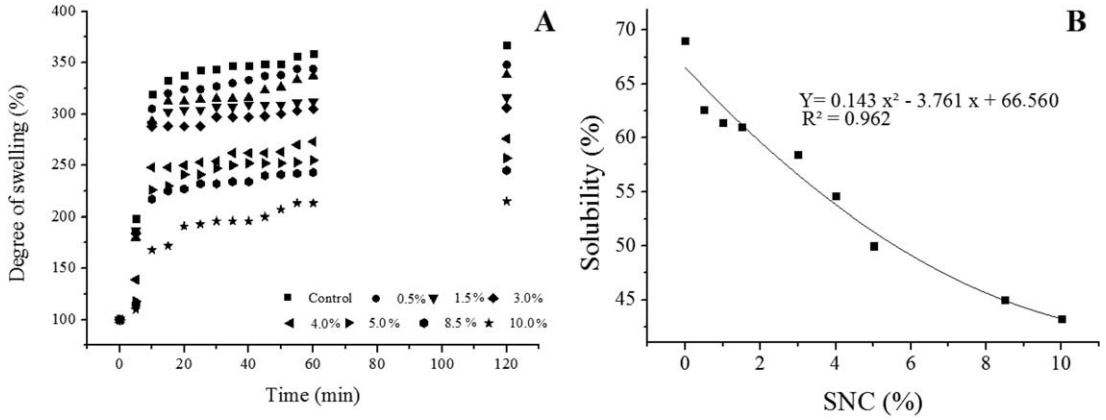

Figure 3. Degree of swelling in water of the cassava starch film (control) and nanocomposite films over time and solubility depending on the cassava starch nanocrystals (CSN) concentration in 120 min.

(20–120 min) in water reduces between 20% and 35% due to the tridimensional network formed by hydrogen connections between matrix:nanocrystal. The phenomenon can be ascribed to the formation of a rigid three-dimensional starch nanocrystal network (due to the strong hydrogen bonding between the starch particles) which prevents swelling of the matrix.[6]

As CSN concentration increased, the solubility of the films in water decreased [Figure 3(B)], following the quadratic model ($R^2 = 0.962$). The presence of nanoparticles increased the stability of the starch films in water, creating a physical barrier to water entry, since nanoparticles are less hydrophilic that starch.[30] The higher RCI (46%) of the CSN [Figure 2(A)], when compared with the granular starch, can allow a more rigid network to be established, formed of hydrogen connections.

Table I shows T_g and T_m values obtained from DSC curves and T_{onset} of the main thermal events obtained from differential thermogravimetry of films, identifying similar behaviors independently from the concentration of CSN. The incorporation of CSN provided an increase in the T_g (from −22.35 to −31.17 °C), which fluctuated depending on the concentration of CSN. The highest value of this interval was obtained with 3.0% of CSN. A single T_g value may indicate that there was no separation of amylose and amylopectin macromolecules from the starch. The presence of nanocrystals can influence the T_g values of the nanocomposites in opposite ways. Nanocrystals can induce a restricted mobility of the polymer chains, thus resulting in changes in T_g at higher temperatures. Conversely, nanocrystals, from certain nanocrystals concentration, may decrease the density of crossed connections in the polymeric matrix, due to clustering.[31]

The T_m of the control film was 233.87 °C. Variations are also found in this parameter depending on the CSN concentration incorporated, varying from 124.11 to 240.94 °C, with the highest value for this interval being obtained in the nanocomposite with 4.0% CSN (Table I). Decreases of approximately 50% in T_m values were obtained for nanocomposites incorporated with 8.5% and 10% of CSN. The reduction in nanocomposites fusion temperatures can facilitate the processability of these materials by extrusion. Dai *et al.*[24] and Chen *et al.*[30] reported a higher T_m for films containing starch nanoparticles compared to films without nanoparticles, indicating a strong interaction between nanoparticles and the polymeric matrix.

TGA (Table I) showed a similar behavior for composite films. The initial weight loss of all samples (T_{onset} = 93–97 °C) is due to water evaporation. The mass loss in the second and third event

Table I. DSC and TGA results obtained for films nanocomposite.

	DSC		TGA thermal events (mass loss %)		
CSN	T_g (°C)	T_m (°C)	T_{onset} I (°C)	T_{onset} II (°C)	T_{onset} III (°C)
0.0[a]	−32.58	233.87	96 (20.00)	152.86 (23.88)	292.16 (48.95)
0.5	−26.68	230.59	95 (18.46)	153.82 (26.04)	294.45 (49.71)
1.0	−30.14	236.47	97 (16.30)	151.87 (22.34)	293.43 (53.98)
1.5	−24.86	152.50	97 (14.70)	153.57 (22.34)	294.45 (49.71)
3.0	−22.35	142.22	95 (18.46)	150.57 (30.87)	294.43 (48.64)
4.0	−25.15	240.94	91 (15.53)	152.86 (27.43)	295.46 (53.48)
5.0	−24.82	230.11	95 (17.38)	153.87 (31.44)	293.43 (47.05)
8.5	−31.17	124.11	96 (17.38)	148.54 (27.43)	294.45 (48.32)
10.0	−27.05	124.51	93 (19.80)	153.87 (24.70)	294.45 (48.95)

CSN, cassava starch nanocrystal; T_g, glass transition temperature; T_m, melting temperature.
[a] Control.

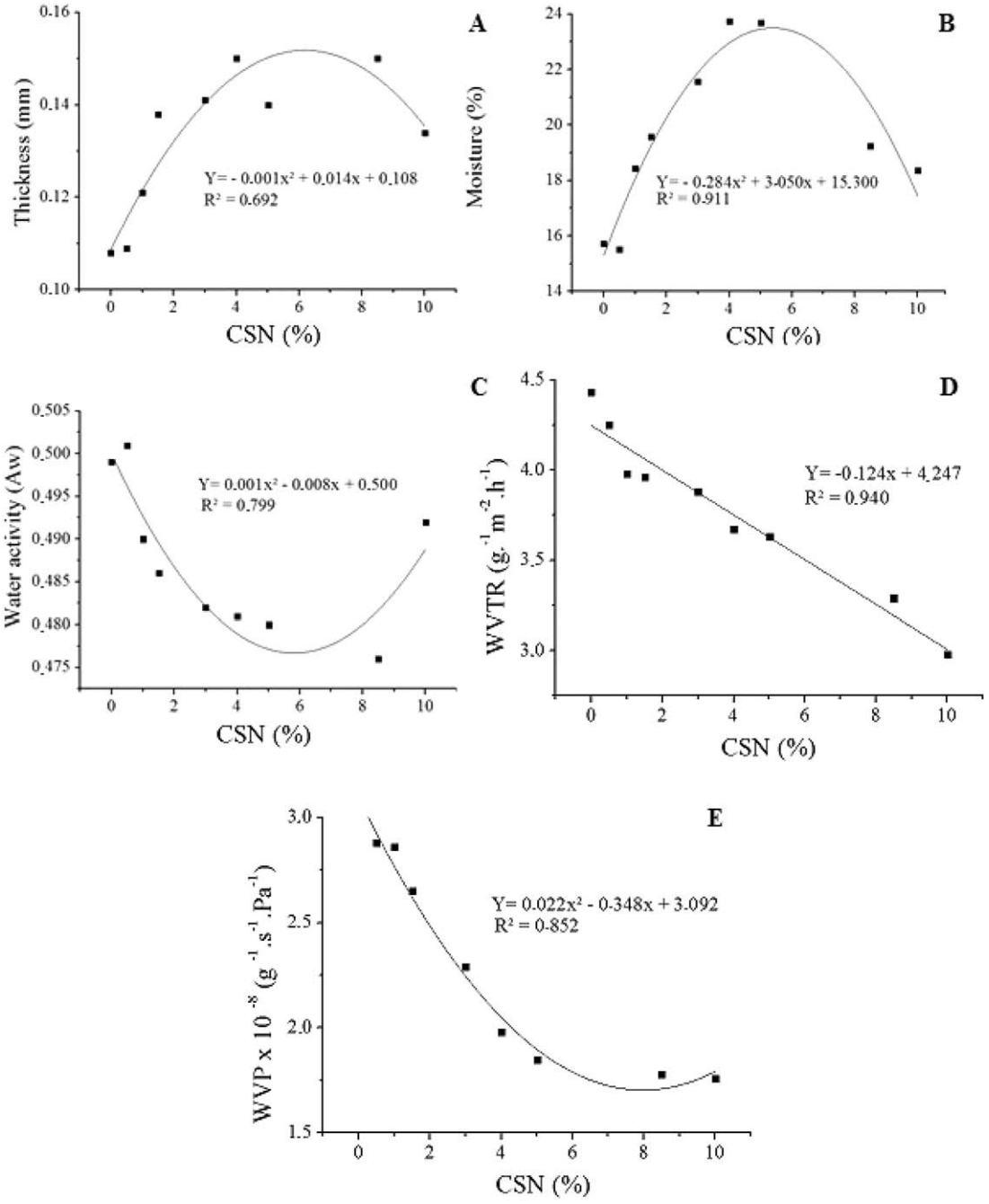

Figure 4. The effect of cassava starch nanocrystals (CSN) concentration on thickness, moisture, water activity, water-vapor transmission rate (WVTR), and water vapor permeability (WVP) of nanocomposites and control films.

(T_{onset} II = 148.54–153.87 °C and T_{onset} III = 293.43–295.46 °C) corresponds to a complex process that includes dehydration of saccharide rings and depolymerization.[32] The TGA analysis showed that all cassava starch films reinforced with CSN are stable up to ~290 °C, with a maximum decomposition at approximately 340 °C. The results showed that loss of mass of the control film was relatively similar than in the films reinforced with CSN, indicating that the addition of CSN does not change the thermal stability of cassava starch films.

The thickness control of films processed through casting depends a lot on the viscosity of the filmogenic solution, and small variations are expected. Incorporating CSN into the cassava starch films resulted in significant alterations ($P < 0.05$) in the thickness of the nanocomposites [Figure 4(A)]. The values varied from 0.108 mm in the control film up to 0.150 nm in the films containing 4.0% and 8.5% CSN, decreasing to 0.130 mm with 10% CSN. Adjustment via the regression analysis shows quadratic behavior between thickness and CSN concentration ($R^2 = 0.692$). The increases may be related with the hydrophilic nature of CSN associated with water sorption, and the effect of the reduction with greater interaction between starch:nanocrystals.[33]

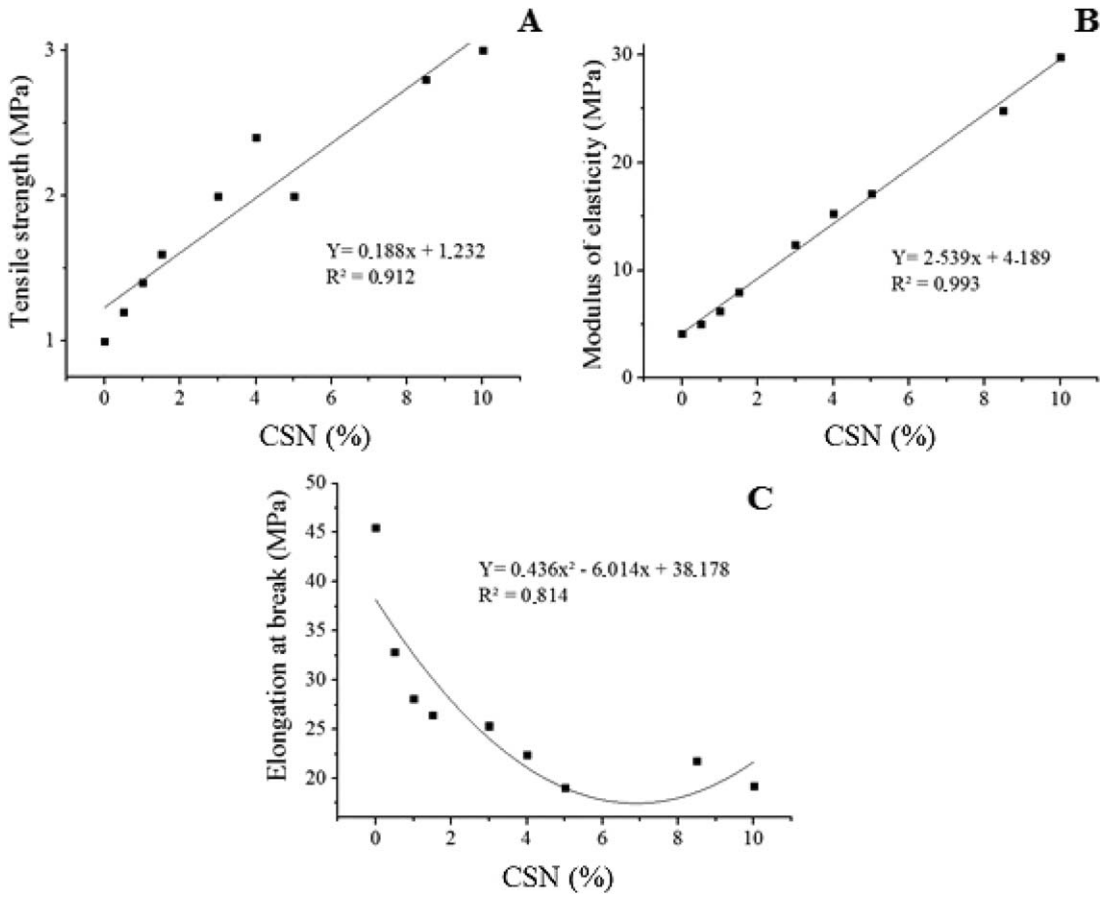

Figure 5. The effect of cassava starch nanocrystals (CSN) concentration on tensile strength, modulus of elasticity, and elongation at break of nanocomposites and control films.

The adjustments of the equations of the experimental points for the dependent variables moisture and water activity (Aw), in function of the independent variable, are related in Figure 4(B,C). The interval of CSN concentration tested significantly influenced ($p < 0.05$) these nanocomposite properties, resulting in quadratic behaviors with high determination coefficients ($R^2 = 0.962$ and $R^2 = 0.799$). The moisture values varied from 15% to 24% with significant differences ($p < 0.05$), similar to those obtained by Condés *et al.*[23] for films containing corn starch nanocrystals obtained by acid hydrolysis, with a polymeric matrix from the same source (15%–22%).

The values for WVP rate (WVPR) and WVP of the films ranged from 2.98 to 4.25 g m^{-2} h^{-1} and 1.76 to 2.88 × 10^{-8} g^{-1} s^{-1} Pa^{-1}, respectively, depending on the concentration of CSN [Figure 4(D,E)]. With 10% of incorporated CSN, there were maximum decreases of 80% and 50% in WVPR and WVP, respectively. This may be due to a good dispersion of the nanocrystals in the starch matrix, resulting in more compact films. WVP showed a quadratic behavior while WVPR a linear behavior in function of the CSN concentration, with high coefficients of determination ($R^2 = 0.852$ and $R^2 = 0.940$, respectively), thus causing a satisfactory adjustment in the second-order regression model with the experimental data.

Theoretically, according to the Fick diffusion and Henry sorption laws, the WVP varies inversely to film thickness.[34] This influence existed since WVP and thickness values presented a coefficient of determination of $r^2 = 0.68$, thus abiding by the aforementioned laws.

Garcia *et al.*[5,35] reported 40% decreases in WVP of cassava starch nanocomposites:waxy maize starch nanoparticles (0.0%–5.0%) and in cassava starch:nanoparticles of the same matrix (2.5%), respectively. Fan *et al.*[36] found that the WVPR and WVP of films of corn starch:corn starch nanocrystals (0.0%–5.0%) decreased significantly ($p < 0.05$) from 4.21 to 3.04 × 10^{-8} g^{-1} s^{-1} Pa^{-1} and from 5.14 to 4.25 g m^{-2} h^{-1}, respectively. In this study, there were no significant differences ($p > 0.05$) in WVP values from 5% of CSN, indicating a stable distribution and dispersion of nanocrystals. Li *et al.*[10] also reported that, with 5% corn starch nanoparticles, WVP of pea starch films reached a minimum; above this value it increased, possibly due to nanoparticle clustering allowing migration of water molecules. With a lower nanoparticle content, there is better dispersion in the films and less clustering, thus making the passage of water difficult and subsequently reducing permeability until a particular nanocrystal concentration.[4]

The incorporation of CSN into cassava starch films resulted in changes in the mechanical properties of the resulting nanocomposites (Figure 5). The tensile strength and the modulus of elasticity of the nanocomposites showed significant differences ($p < 0.05$) and increased with the concentration of CSN while elongation at break decreased.

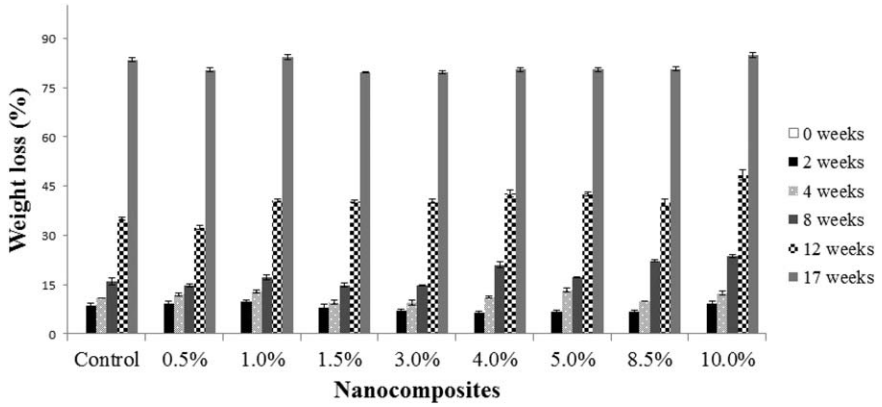

Figure 6. Biodegradability of nanocomposites with different concentration of cassava starch nanocrystals (cassava starch nanocrystals, CSN 0.5%–10.0%).

Based on the linear regression analysis [Figure 5(A)], it is verified that the increase in tensile strength of the films was proportional to the increase in CSN concentration ($R^2 = 0.912$), with a maximum increase of approximately 200% (10.0% CSN) in relation to the control. With the increase in CSN, the material became less ductile, with a consequent increase in tensile strength and decrease in deformation. Thus, the film with 10% CSN presents a more rigid material in comparison with the control film (ductile). Ductile materials experiment greater deformations before rupturing, while the rigid ones show much smaller deformations.[37] Li *et al.*[10] report tensile strength of 9.96 MPa for films with 5.0% pea starch nanoparticles and a 72.90% increase in relation to the control. At the same time, the elongation at break decreased by at least 12.58%.

The linear increase in tensile strength in function of the increase in CSN concentration can result in good dispersion of these in the polymeric matrix, as a result of the transfer of crystal tension to the polymer, but also due to the chemical similarity between the crystals and cassava starch and the intrinsic adhesiveness in the crystal: matrix interface. The denser and more rigid structure of the starch nanocrystals, the uniform distribution, and the manometric dimensions, result in strong interactions with different hydrophilic matrices.[30,38] In this context, Le Corre *et al.*[4] reported that these effects are highly dependent on the nanocrystal concentration interval, and in many cases incorporating nanoparticles into nanocomposite film results in an increase in tensile strength and modulus of elasticity, associated at decrease in the elongation percentage.[11]

Increase in the values of modulus of elasticity of the nanocomposites proportional to the concentration of CNS was evidenced ($R^2 = 0.993$) [Figure 5(B)]. Formulations with 8.5% and 10% of CSN showed increases of 480% and 616%, respectively, compared to the control. Cassava starch films: 10% of CSN from a same matrix, with a tensile strength of 3.0 MPa and a modulus of elasticity of 45 MPa, may be obtained.

The elongation at break presented quadratic behavior in function of the CSN concentrations with a high determination coefficient ($R^2 = -0.814$), [Figure 5(C)]. The formulations with 4.0% and 10.0% CSN presented the greatest reductions (51.58%) when compared with the control. The effect of the reduction in elongation at break was expected, due to the increase in film rigidity. The decrease in nanocomposite elongation is a known phenomenon and is related with differences in rigidity resulting from the interactions between matrix and processing agents.[24]

Figure 6 shows the results from the nanocomposite biodegradability test over 17 weeks of exposure, simulating disposal in the environment. A large percentage of loss of film mass is found over the course of monitoring. Independent of CSN concentration, the size of loss of film mass was similar, varying from 79% to 84%, and the film with 10% CSN presented the greatest percentage of degradation, probably due to greater microorganism access.

Condés *et al.*[23] also showed that loss of mass was similar for corn starch films, with and without corn starch nanocrystals, reaching values between 80% and 90% total biodegradation after 3 weeks. According to Jayasekara *et al.*,[39] the main change that a degradable polymer experiences is a decrease in molecular mass originating in smaller molecules due to microorganism action, especially bacteria and fungi.

CONCLUSIONS

Acid hydrolysis of cassava starch resulted in nanocrystals with the potential for improving nanocomposite film properties, due to their nanometric size, and higher crystalline index compared to native starch. It was verified that CSN concentration significantly influenced mechanical and barrier properties, as well as the water activity and film solubility values of the films of starch:glycerol:CSN/4.0:2.1:1–10 processed through casting. The traction resistance and elastic modulus of the films experienced a linear influence of CSN concentration, while the other parameters resulted in quadratic relations. The film with 10% CSN presented a 43% reduction in WVP, associated with increases of 200% in traction resistance and 616% in elastic modulus, compared with the control. Hydrolysis of part of the cassava starch into nanocrystals resulted in nanoreinforcement of the films due to good compatibility and interaction between both, without any influence on biodegradability, which was 80% after 17 weeks of exposure. Because starch nanocrystals were able to improve key properties of the films, the results obtained here can pave the route for the development and large-scale production of novel biodegradable packaging materials.

ACKNOWLEDGMENTS

The authors are grateful to CAPES (MINCYT 993/2014 process 23038001220/2014–32), and to FAPESB (RED 0017/2013) for the financial subsidy, and also to CAPES for the masters scholarship.

REFERENCES

1. da Silva, J. B. A.; Pereira, F. V.; Druzian, J. I. *J. Food Sci.* **2012**, *77*, N14.
2. Seligra, P. G.; Moura, L. E.; Famá, L.; Druzian, J. I.; Goyanes, S. *Polym. Int.* **2016**, *65*, 938.
3. Moreno, O.; Diaz, R.; Antares, L.; Chiralt, A. *Polym. Int.* **2016**, *65*, 905.
4. Le Corre, D.; Bras, J.; Dufresne, A. *Biomacromolecules* **2010**, *11*, 1139.
5. Garcia, N. L.; Ribba, L.; Dufresne, A.; Aranguren, M. I.; Goyanes, S. *Macromol. Mater. Eng.* **2009**, *294*, 169.
6. Dufresne, A.; Castaño, J. *Starch/Staerke* **2016**, *68*, 1.
7. Santana, J. S.; Rosário, J. M.; Pola, C. C.; Otoni, G. C.; Soares, N. F. F.; Camilloto, J. P.; Cruz, R. S. *J. Appl. Polym. Sci.* **2017**, *134*, DOI: 10.1002/app.44637.
8. Xu, Y.; Scales, A.; Jordan, K.; Kim, C.; Sismour, E. *J. Appl. Polym. Sci.* **2016**, *134*, DOI: 10.1002/app.44438.
9. Teodoro, A. P.; Mali, S.; Romero, N.; De Carvalho, G. M. *Carbohydr. Polym.* **2015**, *126*, 9.
10. Li, X.; Qiu, C.; Ji, N.; Sun, C.; Xiong, L.; Sun, Q. *Carbohydr. Polym.* **2015**, *121*, 155.
11. Kim, H. Y.; Park, S. S.; Lim, S. T. *Colloids Surf. B* **2015**, *126*, 607.
12. Angellier, H.; Choisnard, L.; Molina-Boisseau, S.; Ozil, P.; Dufresne, A. *Biomacromolecules* **2004**, *5*, 1545.
13. Kim, H. Y.; Park, D. J.; Kim, J. Y.; Lim, S. T. *Carbohydr. Polym.* **2013**, *98*, 295.
14. Nara, S.; Komiya, T. *Starch/Staerke* **1983**, *35*, 407.
15. Sriupayo, J.; Supaphol, P.; Blackwell, J.; Rujiravanit, R. *Carbohydr. Polym.* **2015**, *62*, 130.
16. American Society for Testing and Materials (ASTM). *ASTM (Am. Soc. Test. Mater.) Data Ser.* **2010**.
17. American Society for Testing and Materials (ASTM). *ASTM (Am. Soc. Test. Mater.) Data Ser.* **2003**.
18. Leite, M. C.; Furtado, C. R.; Couto, L. O.; Oliveira, F. L.; Correia, T. R. *Polimeros* **2010**, *20*, 339.
19. American Society for Testing and Materials (ASTM). *ASTM (Am. Soc. Test. Mater.) Data Ser.* **2009**.
20. Rajeswari, L. S.; Moorthy, S. N.; Rajasekharan, K. N. *J. Root Crops* **2015**, *41*, 49.
21. Lamanna, M.; Morales, N. J.; García, N. L.; Goyanes, S. *Carbohydr. Polym.* **2013**, *97*, 90.
22. Sun, Q.; Gong, M.; Li, Y.; Xiong, L. *Carbohydr. Polym.* **2014**, *111*, 133.
23. Condés, M. C.; Añón, M. C.; Mauri, A. N.; Dufresne, A. *Food Hydrocolloids* **2015**, *47*, 146.
24. Dai, L.; Qiu, C.; Xiong, L.; Sun, Q. *Food Chem.* **2015**, *174*, 82.
25. Angellier, H.; Putaux, J. L.; Molina-Boisseau, S.; Dupeyre, D.; Dufresne, A. *Macromol. Symp.* **2005**, *221*, 95.
26. Dufresne, A. *Molecules* **2010**, *16*, 4111.
27. Shahrodin, M.; Shazrynda, N.; Rahmat, A. R.; Arsad, A. *Adv. Mater. Res.* **2015**, *1113*, 446.
28. Lecorre, D.; Bras, J.; Dufresne, A. *Carbohydr. Polym.* **2012**, *87*, 658.
29. Freitas, R. A.; Paula, R. C.; Feitosa, J. P. A.; Rocha, S.; Sierakowski, M. R. *Carbohydr. Polym.* **2004**, *55*, 3.
30. Chen, Y.; Cao, X.; Chang, P. R.; Huneault, M. A. *Carbohydr. Polym.* **2008**, *73*, 8.
31. Azizi Samir, M. A. S.; Alloin, F.; Dufresne, A. *Biomacromolecules* **2005**, *6*, 612.
32. Aji, P.; Mathew, A. D. *Biomacromolecules* **2002**, *3*, 609.
33. Stading, M.; Rindlav-Westling, A.; Gatenholm, P. *Carbohydr. Polym.* **2001**, *45*, 209.
34. Martin-Polo, M.; Mauguin, C.; Voilley, A. *J. Agric. Food Chem.* **1992**, *40*, 407.
35. Garcia, M. A.; Martino, M. N.; Zaritzky, N. E. *J. Food Sci.* **2000**, *65*, 941.
36. Fan, H.; Ji, N.; Zhao, M.; Xiong, L.; Sun, Q. *Food Chem.* **2016**, *192*, 865.
37. Ritchie, R. O. *Nat. Mater.* **2011**, *10*, 817.
38. Viguié, J.; Molina-Boisseau, S.; Dufresne, A. *Macromol. Biosci.* **2007**, *7*, 1206.
39. Jayasekara, R.; Harding, I.; Bowater, I.; Lonergan, G. *J. Polym. Environ.* **2005**, *13*, 231.